Properties of polyurethane oligomeric blends *versus* high molecular weight block copolymers

Kirk K. S. Hwang*, Shaow B. Lin, Sun Yuan Tsay† and Stuart L. Cooper
Department of Chemical Engineering, University of Wisconsin, Madison, WI 53706, USA
(Received 18 July 1983)

Segmental compatibility has been investigated in both oligomeric polyurethane blends and polyurethane block copolymers. The block copolymers are formed by linking a hard segment, composed of three MDI and two butane diol units on average with various macroglycols. The monodisperse oligomeric hard segment, H_3, with its chain ends reacted with ethanol is used as the urethane component in blends with macroglycols. The macroglycols used in both the blend and block copolymer systems include polyethylene oxide (PEO), polypropylene oxide (PPO), polytetramethylene oxide (PTMO), and polybutadiene (PBD). Blends of H_3 and PEO form a eutectic at a weight ratio of $\approx$20/80 (H_3/PEO) with a $T_{m,e}$=34°C. H_3 and PTMO blends also give rise to a eutectic composition at $\approx$20/80 (H_3/PTMO) but with a $T_{m,e}$=10°C. Both PPO and PBD mix with H_3 to form a crystalline–amorphous blend. The miscibility of H_3 and the soft segments at the melting point of H_3 is in the order of PEO> PTMO> PPO> PBD. In the block copolymer systems, stress–strain and dynamic mechanical testing indicate that the block copolymerization of a hard segment with each soft segment results in a microphase separated elastomer as expected. The extent of phase separation increases in the order of PBD> PTMO> PPO> PEO which is coincident with the trend predicated by the application of Hilderbrand's solubility parameter concept. All the soft segments used occur in an amorphous phase in the block copolymers while PEO and PTMO crystallize in a blend with H_3. The differences between the properties of the blends and block copolymers suggest that the phase separation, segment crystallization and domain coalescence are substantially restricted by the urethane–polyol junction points.

(Keywords: polyurethanes; block copolymers; model compounds; phase diagrams; compatibility; segmental interaction)

INTRODUCTION

The domain structure which results from phase separation of hard and soft segments in polyurethane block copolymers is well recognized as the principal feature controlling the properties of this class of thermoplastic elastomers. The driving force for phase separation is segmental incompatibility and the factors which influence this include segment polarity, length and crystallizability, potential for soft segment–hard segment interaction such as hydrogen bonding, overall sample composition and molecular weight.

It has generally been observed that longer block lengths result in higher degrees of phase separation[1-5], higher hard segment content results in more hard segments mixed into the soft phase[2,3,5], and that polar soft segments which form strong interactions such as hydrogen bonding with the hard segment exhibit a higher degree of phase mixing[4,6,7].

The common macroglycols used as polyurethane soft segments include polyester and polyether polyols. Polybutadiene (PBD) and polyisobutylene (PIB) macroglycols may also be used as the soft segment in polyurethanes with the realization that without any potential for hydrogen bonding they tend to form a highly phase separated solid-state structure[10-11]. Polyester soft segments are generally more compatible with urethane hard segments than polyether soft segments as the strength and degree of hard segment–soft segment hydrogen bonding is greater for the ester carbonyl group compared to the ether oxygen[12,13]. Among polyether macroglycols, Chang and Wilkes[14] reported that polypropylene oxide (PPO), which contains an extra methyl group compared to polyethylene oxide (PEO), possesses a lower dipole moment, weaker dispersion forces and a lower tendency toward hydrogen bonding than PEO and was thus more incompatible with the hard segments. Recently, Hwang *et al.*[15] studied the phase diagrams of urethane model hard segment blends with different polyether macroglycols (PEO, PPO and PTMO), and reported that phase separation persisted until melting of the urethane compound in each case. Earlier, Lockwood *et al.*[16] studied polyurethane and ethylene oxide–propylene oxide copolymer (P(EO/PO)) blends and found that the P(EO/PO) copolymer was immiscible with a crystallizable MDI/BD polyurethane. The copolymers possessed a one-phase morphology when blended with an amorphous polyurethane (MDI/dipropylene glycol). It appears that the compatibility favoured by intersegmental interaction is markedly affected by the hard segment crystallization. Lockwood also found that blends of pure PPO and polyurethanes result in a two-phase morphology regardless of hard segment crystallinity, suggesting PPO had

* Present address: 3M Company, Life Science Sector Laboratory, St. Paul, MN, USA
† Permanent address: Cheng-Kung University, Taiwan ROC

0032-3861/84/070947-09$03.00

much lower compatibility with polyurethanes than PEO. This observation is consistent with the conclusions of Chang and Wilkes on PEO- and PPO-based polyurethane block copolymers.

In the present study, segmental compatibility is investigated in both blend and block co-polyurethane systems. A hard segment composed of 3 MDI units reacted with butandiol was linked with various soft segments to form the segmented copolymers. The same oligomeric hard segment with its chain ends reacted with ethanol, coded as H_3, was used as the oligomeric component of various blend systems. The soft segments used for both the blends and block copolymer systems included PEO (100 MW), PPO (1050 MW), PTMO (990 MW) and PBD (1970 MW), where only PEO and PTMO were crystallizable. PBD was the only macroglycol studied that had no possibility of forming hydrogen bonds with the hard segments. The effect of the soft segement type on the physical properties of both the blends and block copolymer systems have been compared and the influence of the linkage between the hard and the soft segements on component miscibility and sample morphology are described in this paper.

EXPERIMENTAL

The details of the synthesis of the hard segment model compound H_3 and the block copolymers has been published elsewhere[17]. The polyols used were hydroxyl terminated-polybutadiene (1970 MW) (PBD) of functionality 1.9, provided by Japan Synthetic Rubber Co., polytetramethylene oxide glycol (990 MW) (PTMO) obtained from Quaker Oats, polypropylene oxide glycol (1050 MW) (PPO) provided by BASF Wyandotte, and polyethylene oxide glycol (1000 MW) obtained from Aldrich Chemical Co.

Blends of H_3/PBD, H_3/PTMO, H_3/PPO and H_3/PEO were prepared from dilute solution using a solvent mixture of DMA and THF (1:3 vol/vol). The solvent was slowly evaporated at room temperature and the samples then further dried under vacuum for 2 weeks at 25°C. Films of the H_3/polyol-based block copolymers for physical testing were prepared by spin casting, followed by drying in a vacuum oven at ≈55°C for one week.

Infrared survey spectra were recorded on a Nicolet FTIR-7199 infrared spectrophotometer at a resolution of $2\,cm^{-1}$. The i.r. survey spectra were obtained from films cast from a solvent mixture of DMA/THF (1:3 vol/vol). The i.r. absorbance of C=O region was resolved into free and bonded band peak areas using a non-linear least squares, Laurentzian and Gaussian combination peak fit computer program.

Density measurements were carried out using a pycnometer and ASTM method D-70. The pycnometer was calibrated using mercury as a standard. D.s.c. measurements were carried out using a Perkin–Elmer DSC-2 which was calibrated with mercury and tin standards to ±0.5°C. A fast heating rate of 20°C min^{-1}, was used in the present study because the hard segment model compound, H_3, begins to decompose at temperatures >180°C[21]. All d.s.c. experiments were carried out under a He atmosphere.

Dynamic mechanical data were obtained by using a Rheovibron DDV-II apparatus which was controlled automatically by a LSI-11 mini-computer. Samples were made by spin casting and had thicknesses between 25–250 μm depending on the temperature range being studied. All measurements were carried out under nitrogen at a frequency 110 Hz at a constant heating rate of 20°C min^{-1}.

Uniaxial stress–strain data were obtained using a table-model Instron tensile testing machine at a crosshead speed of $\approx 12.5\,mm\,min^{-1}$. Samples were spin cast to a thickness of ≈15 mm and stamped out with an ASTM D412 die. The per cent elongation recorded is the true strain determined from benchmarks placed on the sample. The stress was calculated as force/original cross-section area.

RESULTS AND DISCUSSION

H_3–polyol phase diagrams

Blends of hard segment model compound and polyols were prepared from a dilute solution using a solvent mixture of DMA and THF (1:3 vol/vol), which is a good solvent for both H_3 and the polyols.

Differential scanning calorimetry was used to determine the phase diagrams of the blends of the polyols with the hard segment model compound. In each system, the composition ratio of H_3/polyol was varied from 100/0 to 0/100. *Figures 1–4* show the phase diagrams of H_3 with PEO, PPO, PTMO and PBD. Among the soft segments, PEO and PTMO are crystallizable, with melting points at 45°C and 23°C, respectively. The PPO and PBD soft segments are amorphous, with T_g's at −69 and −65°C, respectively. Based on the thermal transitions measured from d.s.c., H_3–PEO blends are shown to possess a eutectic phase diagram with a eutectic composition, at H_3/PEO (20/80). The melting point of the eutectic mixture was ≈34°C. As no eutectic melting was observed for the sample with a composition of H_3/PEO (95/5), a limited solid solution phase (designated as β) is suggested in this region of the diagram. A small solid solution region (H_3 in PEO) (assigned as α) is also suggested at high PEO content. This was not observed experimentally, most likely because the H_3 content is too low to be detectable. Above the liquidus line, which was taken as the minimum point of the H_3 melting endotherm, PEO and H_3 are assumed to be in a well mixed liquid state. The solidus line (dashed line) in the region rich in H_3 was qualitatively determined based on the melting point onset of the blends. Below the eutectic endotherm, which was determined by the melting onset of the eutectic fraction, H_3 and PEO phase separate into two crystalline forms, (α and β). Compared to the previously reported phase diagrams of the H_1/PEO (1500) system[15], where H_1 only contains one MDI unit and the blends possess a eutectic composition of H_1/PEO (40/60) with $T_{m,e}=31$°C, the H_3/PEO (1000) eutectic composition is at a lower concentration of H_3, and possesses a higher eutectic melting temperature (34°C). This could be caused by several factors including a difference in the interaction parameter χ_{12} of the polyol–hard segment pairs, melting temperatures and ΔH of fusion of both components, and the molar ratios of the components used. As suggested by Nishi[18], if two different crystalline polymers are compatible in the molten state, they will have a common melting point at a certain volume fraction designated as the eutectic. The volume fraction ($\phi_{1,e}$) of component 1 in the eutectic can be expressed as:

$$\phi_{1,e}=(1/2)\left\{1+(\Delta H_{1u}V_{2u}/RV_{1u}\chi_{12})\left[\frac{1}{T^{\circ}_{m\cdot 2}}-\frac{1}{T^{\circ}_{m,1}}\right]\right\} \quad (1)$$

assuming $\Delta H_{1u}/\Delta H_{2u}=(V_{2u}/V_{1u})^2$. The subscripts 1 and 2 identify the polyol and the urethane component, respectively, V_u is the molar volume of the repeat units, $T^\circ_{m,2}$ is the equilibrium melting temperature of urethane component and $T^\circ_{m,1}$ that of polyol. χ_{12} is the Flory–Huggins interaction parameter between the urethane component and a polyol. ΔH_{2u} and ΔH_{1u} are the heat of fusion per mol of urethane repeat unit and of polyol repeat unit, respectively.

Figure 2 shows the phase diagram of the H_3/PTMO (1000) system, which possess a eutectic composition containing 20% H_3 with a $T_{m,e}=10°C$. This is almost identical to that of H_1/PTMO system, the eutectic of which also contains 20% H_1 with a $T_{m,e}\approx 10°C$[15]. Samples with compositions of H_3/PTMO of 95/5 and 90/10 show no eutectic melting, suggesting that a solid solution prevails in the region rich in H_3.

Figure 3 shows a typical crystalline–amorphous phase diagram of the H_3/PPO system. The PPO added was amorphous, having a T_g of $-69°C$. It was found that the melting point of H_3 is not affected by the addition of PPO. Similarly, the PPO glass transition temperature appears at $\approx -69°C$, regardless of the concentration of H_3. This suggests that H_3 and PPO do not mix at the molecular level to any extent. However, when the PPO concentration decreases to $<20\%$, the PPO may occur as a finely divided phase inclusion, the T_g of which is not observable in the d.s.c. experiment.

The H_3/PBD system is similar to the H_3/PPO system exhibiting a crystalline–amorphous phase diagram (*Figure 4*). At each blend composition down to 20% H_3, H_3 possesses the same melting point as it does in the pure state (231°C). The PBD glass transition temperature of $-65°C$ was observed in each blend down to a PBD concentration of 20%. As a general observation, the glass transitions as well as melting endotherms in the H_3/PBD system are sharper and more distinct than they are in the H_3/PPO system. This suggests that PBD is more incompatible with H_3 than PPO.

Compared with the H_1/polyol blends, in which the T_m of H_1 is significantly depressed by the addition of PEO or PTMO, the melting behaviour of H_3 in the H_3/polyol blends is much less sensitive to the presence of polyols.

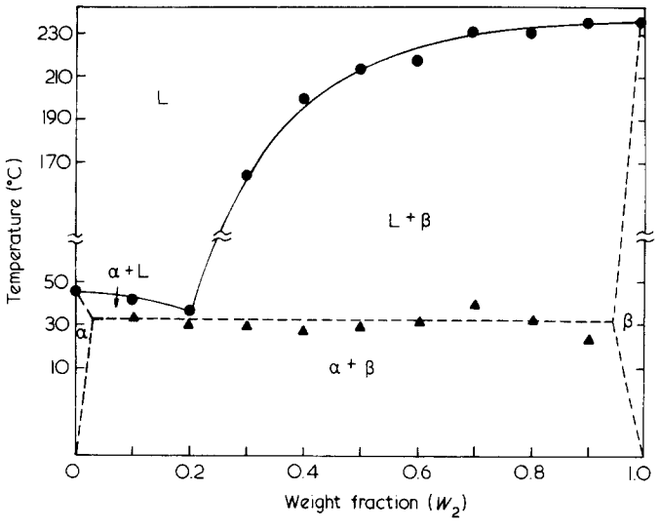

Figure 1 Phase diagram of the H_3/PEO blend system. ●, Liquidus points; ▲, eutectic points. The solidus lines at both ends of the phase diagram are estimated

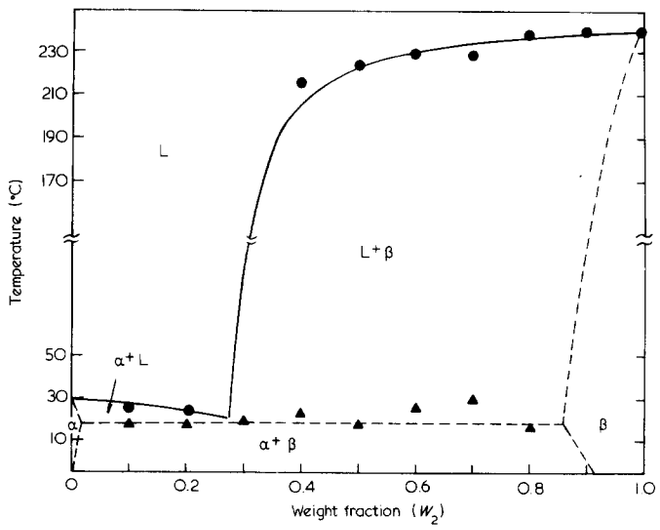

Figure 2 Phase diagram of the H_3/PTMO blend system. ●, Liquidus points; ▲, eutectic points. The solidus lines at both ends of the phase diagram are estimated

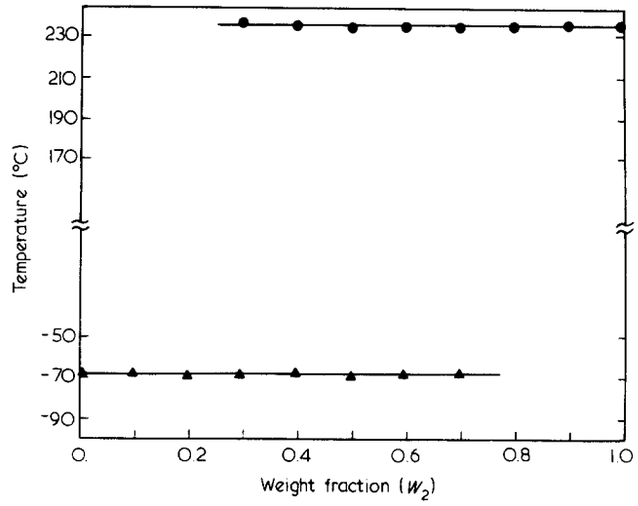

Figure 3 Phase diagram of H_3/PPO blends. ●, Melting points; ▲, glass transition points

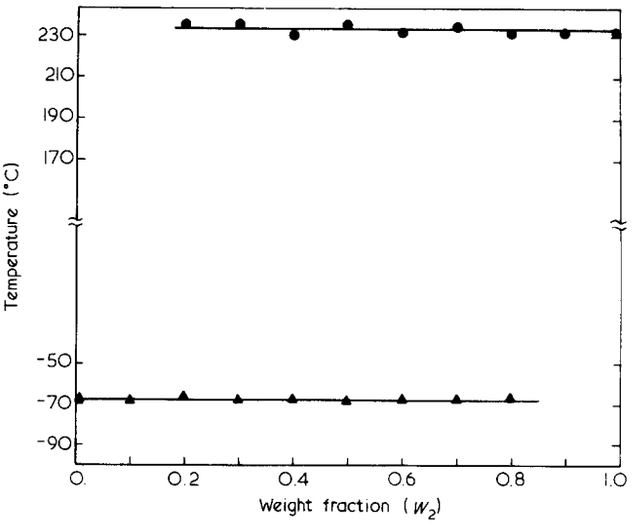

Figure 4 Phase diagram of H_3/PBD blends. ●, Melting points; ▲, glass transition points

This suggests that the excress free energy released during the mixing of H_3 and the polyols is less than that in the H_1/polyol blends.

In an attempt to calculate the interaction densities between H_3 and the polyols, the Scott equation[19] was applied:

$$\frac{1}{T_{m2}}-\frac{1}{T_{m2}^{\circ}}=\frac{RV_{2u}}{\Delta H_{2u}V_{1u}}\left[\frac{\ln\phi_2}{M_2}+\left(\frac{1}{M_2}-\frac{1}{M_1}\right)\phi_1+\frac{BV_{1u}}{RT}\phi_1^2\right] \quad (2)$$

where component 2 is the crystallizable component H_3, T_{m2} and T_{m2}° are the equilibrium melting temperatures of component 2 in the blend and in the pure state, respectively, ΔH_{2u} is the heat of fusion per mol of component 2 repeat unit in the 100% crystalline state, and ϕ_2 is the volume fraction of component 2 in the blend. B is the interaction density, which is related to the Flory–Huggins interaction parameter ($\chi_{12}=BV_{1u}/RT$). The first two terms in the right-hand side of equation (2) represent the usual combinational entropy of mixing. The term containing B includes all other contributions, including the enthalpic interactions between the two components, and also the effect of entropy changes unaccounted for by the simple combinational term[20]. If the combinational entropy terms of equation (1) are neglected, equation (2) reduces to equation (3).

$$\left(\frac{1}{T_{m2}}-\frac{1}{T_{m2}^{\circ}}\right)/\phi_1=\frac{RV_{2u}}{\Delta H_{2u}V_{1u}}\frac{BV_{1u}}{RT}\phi_1 \quad (3)$$

B may then be directly evaluated from the slope of the plot of $\left(\frac{1}{T_{m2}}-\frac{1}{T_{m2}^{\circ}}\right)/\phi_1$ *versus* ϕ_1/T_{m2}.

Figure 5 shows the plot suggested by equation (3) with a listing of slopes and intercepts for each of the four systems studied. A value of 240°C for the T_m° of H_3 was obtained by extrapolating the T_m of the H_3/polyol blends to zero polyol concentration. Based on a ΔH_{2u} of 5.3 Kcal mol^{-1} ($\simeq$22 kJ mol^{-1})[21] for H_3 and the measured densities of H_3, PEO, PPO, PTMO and PBD which were 1.298, 0.986, 1.004, 0.977 and 0.860, respectively, the interaction density between H_3 and each polyol were determined. These are given in *Table 1* where they are compared with corresponding values for the H_1–polyol mixtures[15]. Regarding the H_3–polyol interaction density, PEO and

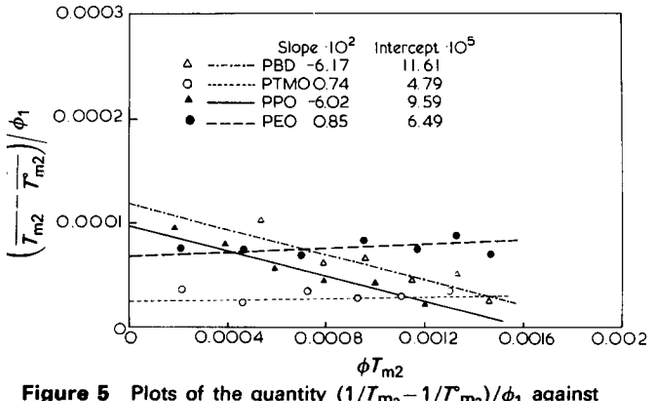

Figure 5 Plots of the quantity $(1/T_{m_2}-1/T^{\circ}_{m_2})/\phi_1$ against ϕ_1/T_{m_2} for H_3/PEO, H_3/PTMO, H_3/PPO and H_3/PBD systems

Table 1 Interaction densities of the model compound blends

Hard segment model compound	B (cal cm^{-3}) PEO	PPO	PTMO	PBD
H_1[a]	−4.67	−1.21	−3.45	–
H_3	−0.20	1.39	−0.17	1.43

[a] The interaction densities (B) between the H_1 and the polyols studied were reported previously[15]

PTMO possess a slightly negative B, while PPO and PBD exhibit positive B values. This suggests that PEO and PTMO are miscible with H_3 molecules at the melting point of H_3, while PPO and PBD are not able to mix with H_3 unless their gain of combinational entropies due to mixing are large enough to overcome the insufficient enthalpic interactions between the hard and soft segment. It is also clearly shown that all of the B values for the H_1/polyol blends are smaller than those for corresponding H_3/polyol systems. As expected, the increase in the hard segment length suppresses compatibility to a large extent. This is largely due to an entropy of mixing decrease caused by the extension of hard segment length. It is noteworthy also that the PEO used in the H_3/PEO blends possessed a molecular weight of 1000 MW while it was 1500 MW in the H_1/PEO blends. It is expected that B for the H_1/PEO system would be smaller than the −4.67 cal cm^{-3} (−19.53 J cm^{-3}) reported if PEO of 1000 MW was used.

Block copolymers

In an attempt to study the effect of block copolymerization on the morphology of the urethane–polyol mixtures, a series of block copolymers based on the same polyols used for the blends was prepared. It is generally accepted[22-23] that the presence of covalent bonds between different segments in a block copolymer causes an appreciable loss in configurational entropy of mixing and thus phase separation is usually observed at relatively low segment molecular weights. In the present study, i.r., d.s.c. and dynamic mechanical testing were used to investigate the microphase separation in the block copolymers.

Infra-red spectroscopy

I.r. has been shown to be an effective technique to evaluate the extent of phase separation in segmented polyurethanes. Previous studies[25] showed that nearly all the NH groups in polyether polyurethane block copolymers are hydrogen bonded. However, it appears that only a portion of the urethane carbonyls are involved in hydrogen bonding as the N–H proton acceptor. It has been postulated that substantial hydrogen bonding of the NH groups occurs with the ether oxygens of the polyether soft segments[25]. Hydrogen bonding between the NH and C=O groups is normally assumed to take place in hard segment aggregates or domains, while hydrogen bonding between NH groups and ether oxygens is assumed to take place at the domain interface, as well as between urethane segments dissolved in the rubbery phase and the soft segments.

Figure 6 shows the i.r. spectra of the four model polymers in the spectral regions of interest. In each polyether based polyurethane, the NH band in the region

of 3200–3500 cm^{-1} appears to be highly hydrogen bonded, as the bonded NH peak at 3300 cm^{-1} predominates and the free NH peak at 3460 cm^{-1} appears as a small shoulder, if at all. The PBD based polyurethane shows a more prominent free NH shoulder at 3460 cm^{-1}. This is likely due to urethane segments which are surrounded by PBD in the soft segment phase. In the region of 1650–1750 cm^{-1}, the C=O absorption band for each material splits into two peaks. The hydrogen bonded C=O absorption peak centres at $\approx$1700 cm^{-1} while the free C=O absorption peak appears at 1732 cm^{-1}. Previous studies[26] suggest that the extinction coefficients for both bonded and free carbonyl bands are approximately the same. As shown in equation (4), the fraction of bonded C=O groups can be approximated from the ratio of the area of the curve-resolved bonded C=O absorption band to the total area of the 1700 and 1732 cm^{-1} absorptions:

$$\%\,\text{Bonded C=O} = \frac{A_{1700}}{A_{1700}+A_{1732}} \qquad (4)$$

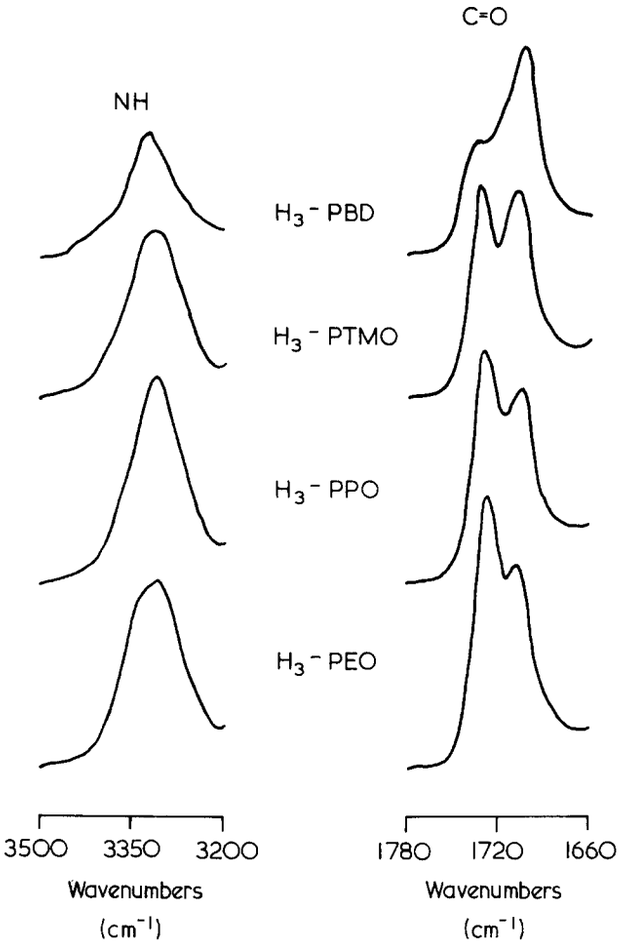

Figure 6 Infra-red spectra of the polyurethane block copolymers with varying soft segment chemistry (PBD, PTMO, PPO and PEO) in the NH and C=O stretching regions

Table 2 shows that the extent of phase separation in the MDI based polyurethanes decreases in the order of PBD, PTMO, PPO and PEO for the macroglycols used in the study. This can be explained by the increase in ether content of the polyols which from zero in PBD to a rather high level in the PEO based polyurethanes as indicated in column four of *Table 2*. Column 5 of *Table 2* gives the weight fraction of hard segment in aggregates or domains. This calculation is based on the assumptions that the fraction of bonded C=O groups is representative of aggregated hard segments and that no soft segment material is dissolved in the hard segment domains.

Thermal analysis

D.s.c. was used to study thermal transitions of the block copolymers. The T_g's of the pure soft segements were −65, −85, −69 and −67°C for PBD, PTMO, PPO and PEO, respectively. The T_m of H_3 was 233°C. As the hard segments and soft segments are linked to make a block copolymer, the thermal transitions of both constituents are altered depending on the degree of phase mixing and overall sample morphology. *Figure 7* shows the d.s.c. thermograms of the block copolymers studied. The soft segment phase T_g and hard segment phase T_m are given in *Table 3*. The PEO-based polyurethane, the components of which are both crystallizable before block copolymerization, shows only one T_g for the soft segment phase at −16°C with no trace of melting for either constituent. This indicates that the PEO-rich phase is in an amorphous state and contains a considerable fraction of solubilized hard segment. This conclusion is also supported by the infra-red results described previously (*Table 2*) suggesting that 56% of the hard segments are dissolved in the PEO soft segment phase. The rest of the hard segments may form small aggregates which could be too small in size and or too low in hard segmented content to exhibit detectable thermal transitions. Similar to the

Table 2 Infra-red determination of the hydrogen-bonded carbonyl fraction of the polyurethane block copolymers

Sample	MDI (wt%)	Hard segment[a] (wt%)	$\frac{[-O-]^b}{[C=O]}$	$\frac{[A_{C=O,b}]}{[A_{C=O,b}]+[A_{C=O,f}]}$	Hard segments[c] in the hard domain (wt%)	Relative[d] hard segment concentration in the soft phase
H_3–PBD	26	35	0	70	25	13
H_3–PTMO	39	53	2.3	51	27	36
H_3–PPO	39	52	2.9	46	24	38
H_3–PEO	39	53	3.8	44	23	39

[a] The hard segment in the block copolymer is defined to have the same length as H_3 in the blend
[b] The molar ratio of total ether [–O–] *versus* total urethane [C=O] on the polymer chains
[c] The product of [wt% hard segment] and $[A_{C=O,b}]/[A_{C=O,b}] + [A_{C=O,f}]$, assuming that hard segment domains contain only polyurethane segments
[d] This calculation is based on the assumption that the hard segments possessing free C=O exist in the soft segment rich phase. Thus:

$$\text{Relative hard segment concentration in soft phase} = \frac{\text{wt\% hard segment dissolved in soft segment phase}}{\text{(soft segment wt\%) + wt\% hard segment dissolved in the soft segment phase}} \times 100\%$$

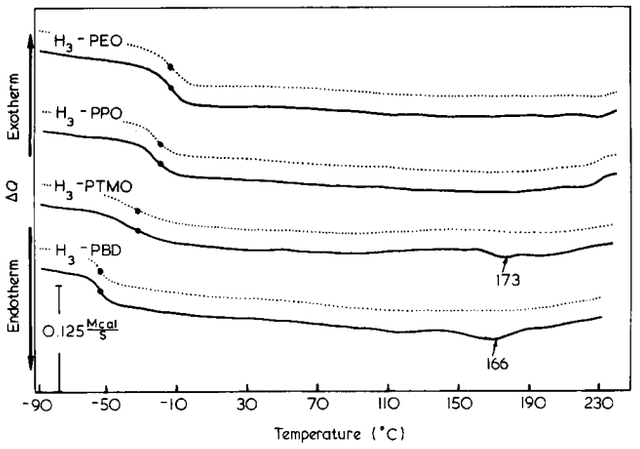

Figure 7 D.s.c. thermograms for the polyurethane block copolymers with varying soft segment chemistry (PBD, PTMO, PPO and PEO). ·····, control; ———, annealed

Table 3 D.s.c. results of the model polyurethane block copolymers

Sample	T_m (°C)	T_g (°C)	Relative weight fraction of hard segment in the soft segment phase	
			From d.s.c.[a]	From i.r.[b]
H_3–PBD	166	–57	11	13
H_3–PTMO	173	–41	37	36
H_3–PPO	–	–23	39	38
H_3–PEO	–	–16	44	39

[a] Calculated based on T_g elevation using the Fox equation
[b] Calculated based on the fraction of non hydrogen-bonded carbonyl absorbance

PEO-based polyurethane, the PPO-based polyurethane exhibits an elevated soft segment glass transition at −23°C and no hard segment melting is observed. I.r. analysis indicated that 54% of the hard segments are dissolved in the soft phase. The PTMO-based polyurethane has a soft segment glass transition temperature at −41°C, and in an annealed sample, a hard segment phase melting endotherm at 173°C. As no variation in the soft segment glass transition was observed after annealing, it may be assumed that the annealing process only improves the hard segment ordering and does not significantly affect the extent of phase separation in the PTMO rich phase. The same annealing treatment (100°C for 5 h) was applied to the PEO- and PPO-based systems but no change in their d.s.c. characteristics upon reheating was observed. This may suggest that there are fewer and smaller hard segment aggregates in the PEO- and PPO-based systems. Finally, the PBD-based polyurethane, in which the hard segments are linked with PBD segments of 1970 MW (the other polyols have MW ≈ 1000) shows a soft segment T_g at −57°C and (after annealing) a melting endotherm at 166°C. No change in the soft segment glass transition temperature upon annealing was observed.

In an attempt to calculate the fraction of hard segments in the soft segment phase from the T_g shift and compare this result to the infra-red analysis, the polyurethane block copolymers were approximated as ordinary random copolymers. This may be justified by the fact that both the hard and soft segment blocks are relatively short, as well as poly disperse. It is then assumed that the elevation of T_g of the soft segment phase is due to the additive effect of the mixed composition and apply the Fox equation, equation (5):

$$\frac{1}{T_g}=\frac{W_1}{T_{g_1}}+\frac{W_2}{T_{g_2}} \tag{5}$$

where T_{g_1} is the glass transition of the pure polyol soft segment (*Table 3*), and T_{g_2} is the glass transition temperature of the MDI/BD hard block. A value of 110°C was used for T_{g_2}[27]. W_2 represents weight fraction of hard segment in the soft segment phase, which increases the glass transition temperature to the observed T_g. The W_2 value for each system calculated using the Fox equation (*Table 3*) shows good agreement with the results from i.r. analysis. The results of both d.s.c. and i.r. show that the miscibility between the polyol soft segments and hard segments in the soft segment rich phase appears to be in the order of PEO > PPO > PTMO > PBD, which is also the order of ether group density in the polyol chain backbone.

In the present case the soft segment-rich phase for each block copolymer is amorphous and thus melting point depression information could not be used to calculate an interaction parameter as was done for the blend system. An alternative method based on the solubility parameter concept, proposed by Fedors *et al.*[28] was used to estimate the χ_{12} in this case:

$$\chi_{12}=\frac{M_1}{\rho_1 RT}(\delta_1-\delta_2)^2=\frac{M_1(\Delta\delta)^2}{\rho_1 RT} \tag{6}$$

where δ_1 and δ_2 are the solubility parameters of the polyol and hard segment, respectively, and ρ_1 and M_1 are the density and molecular weight of the polyol. The solubility parameter, δ_i, of each component are related to the molar energy of vaporization (E_i) and the molar volume V_i as expressed in equation (7):

$$\delta_i=\left(\frac{E_i}{V_i}\right)^{1/2} \tag{7}$$

The change of enthalpy on the mixing of two liquids can be expressed as:

$$\Delta H_M=V_T(\delta_1-\delta_2)^2\phi_1\phi_2 \tag{8}$$

As can be seen from equation (8), the Hilderbrand theory predicts only endothermic heats of mixing. The heat of mixing is zero (athermal, $\chi=0$) when δ_1 and δ_2 are equal, and consequently the mixing process is governed by the entropy change of mixing. It is generally accepted that the mutual solubility of the polymer segments is strongly dependent on having a small difference in the solubility parameters of the given repeat units. A comparison of the repeat unit solubility parameters should provide an approximate guide for estimating the degree of phase separation in the segmented polymer. According to equations (6) and (8), a larger value of $\Delta\delta$ between two different monomers results in a more positive value for both χ (equation (6)) and ΔH_m (equation (8)), and thus promotes phase separation. *Table 4* gives the solubility parameters of monomers for the urethane hard segments, PEO, PPO, PTMO and PBD, respectively. As polyethers can form hydrogen bonds of moderate strength, a correction was made for the ether δ as suggested in the literature[29]. It was found that the $\Delta\delta$ for urethane hard

segment–polyol pairs decreases in the order of PBD > PTMO > PPO > PEO. As suggested by Tobolsky[32], polymers generally become insoluble in a solvent if the $\Delta\delta$ is greater than 2. The $\Delta\delta$ given in *Table 4* indicates that PBD is highly incompatible with the urethane segments, while the miscibility of urethane and polyether in the soft segment-rich phase should increase with increasing ether density. These predictions are consistent with the experimental results obtained from both i.r. and d.s.c. analysis.

As shown in *Figure 7*, melting endotherms at 166 and 173°C were observed for PBD- and PTMO-based polyurethanes. The existence of hard segment crystallinity in these materials can be ascribed to their better phase separation compared to PEO- or PPO-based materials. However, the hard segment melting points of these materials are much lower than those of their blend analogues. One explanation is that the movement of hard segments in the block polymers is largely restricted by their connections to the soft segments resulting in a lower rate and extent of crystallization. In addition, the mixing of hard segments and soft segments at the molecular level elevates the T_g of the soft segment phase. This can further limit the growth of hard segment lamella size by lowering the diffusion rate of hard segments in the soft segment phase.

Dynamic mechanical testing was used to obtain data on the dynamic modulus (*E' and E"*) and internal friction (tan δ) of the block copolymers as a function of temperature. The dynamic loss modulus or tan δ is sensitive to various molecular motions, structural heterogeneities and morphology of multiphase systems. The largest loss peak, designated as the β peak, is associated with the glass transition temperature. In the case of multiphase polyurethane block copolymers, the β peak of the soft segment phase is generally lower in height and broader on the high temperature side than the β peak observed in a pure amorphous polymer. It was also found previously[33,34] that the extent of the β peak height decrease and peak broadening becomes considerable as the hard segment phase changes from isolated or dispersed domains to an interconnected domain morphology. This is because the response of the soft segment phase in a mechanical sense is largely governed by the restraints imposed by the hard segment domains. It has been found that a material with fixed chain architecture and composition, can possess a rubbery modulus that varies from $\approx 10^7$ Pa to $\approx 5 \times 10^8$ Pa as the hard segment domain morphology changes from isolated domains to an interconnected phase morphology. The dynamic modulus above the soft segment T_g increases with increasing volume fraction of hard segment domains as well as the degree of hard segment cohesion.

Figure 8 shows the dynamic mechanical response of the polyurethane block copolymers. A rubbery plateau following the soft segment glass transition region (where storage modulus decreases by two decades) was observed for each sample. This is a typical characteristic for a two-phase segmented elastomer. The glass transition temperatures determined by the position of the β peak maximum (E'' or tan δ) are in the order of PBD > PTMO > PPO > PEO and correlate well with the results obtained from d.s.c. measurements. The rubbery moduli above T_g, e.g. $T_g + 50$°C are in the order PTMO > PEO > PPO > PBD. The low rubbery modulus ($\approx 9 \times 10^7$ MPa) observed for PBD based polyurethane could be ascribed to its lower hard segment content (34 wt%) and longer interdomain spacing due to its greater soft segment length ($M_{PBD} = 2000$). The other polyols (PEO, PPO and PTMO) are of 1000 MW. The rubbery plateau modulus for PTMO-based polyurethane was found to be $\approx 5 \times 10^8$ Pa which is similar to the modulus observed for most styrene–butadiene–styrene triblock polymers in which styrene occurs in a lamellar morphology. It was also found that the dynamic mechanical characteristics of the PTMO-based polyurethane appear similar to that of ET-38, a material which contains a composition similar to H_3–PTMO which was suggested to possess an interconnected hard segment domain morphology[7,33]. According to i.r. and d.s.c. analysis, approximately 50% of the hard segment in the H_3–PTMO sample resides in the soft segment phase so that the volume fraction of the hard segment phase is < 25% assuming the pure hard segment density for the hard segment domain. Based on both Meier[35] and Helfands[36] theory, a hard segment phase with volume fraction < 25% should not be able to form a lamellar or continuous morphology. There may, however, be some unique conformational behaviour of the urethane segmented copolymer which may rationalize this

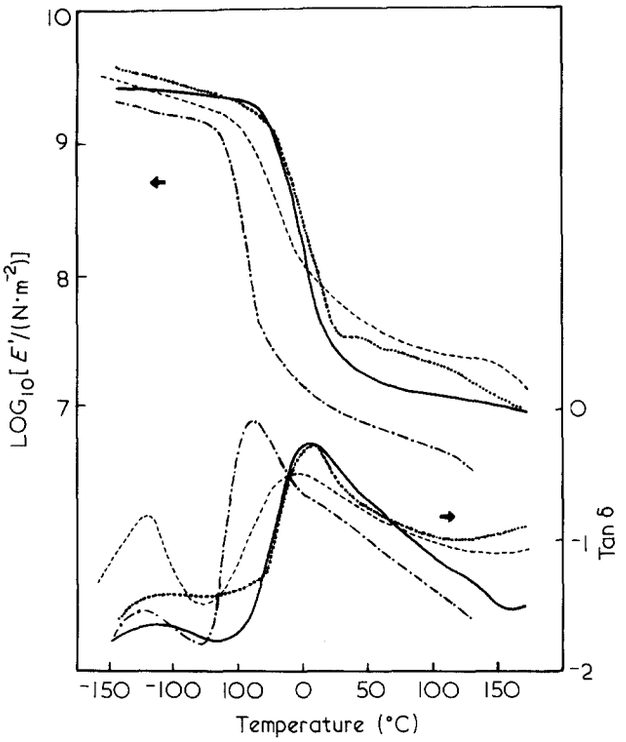

Figure 8 Storage modulus (E') and tanδ curves for the polyurethane block copolymers with varying soft segment chemistry (PBD, PTMO, PPO and PEO). ·····, H_3-PEO; ——, H_3-PPO; – – –, H_3-PTMO; –·–·–, H_3-PBD

Table 4 Solubility parameters of urethane hard segment and polyols

Material	δ [cal cm^{-3}]$^{1/2}$ [a]	$(\Delta\delta)^2$ [cal cm^{-3}]
Urethane	10.0	–
PBD	7.1	8.41
PTMO	8.2	3.24
PPO	8.7	1.69
PEO	11.1	1.21

[a] From refs. 29 and 31
[b] $\Delta\delta = \delta_1 - \delta_2$, where δ_1 is the solubility parameter of the polyol and while δ_2 that of the urethane hard segment

discrepancy. H_3 is a rod-like molecule and with an extended length of ≈ 5 nm[37] while the single PTMO (1000 MW) segment may be assumed to be a random coil with an end to end distance of ≈ 2.8 nm at θ conditions[30]. As the hard segment does appear to be rod-like, there is a good possibility that the hard segment domains or bundles overlap laterally or stack transversely in the soft segment matrix. The hard segment domains could be connected at contact points by strong secondary bonding. In addition, some hard segment domains may be connected by single hard segments forming a 3-dimensional framework. This could explain why the H_3–PTMO block copolymer with only 51% of its hard segments in identifiable 'domains' which may occupy less than 21% by volume of the polymer ($\rho_H \approx 1.29$) exhibits dynamic moduli characteristics of materials with interlocking high modulus domain structures. The same argument for the PTMO-based material may also be applied to explain the high rubbery modulus for the PPO- and PEO- based materials.

Stress–strain measurements

The results of uniaxial stress–strain tensile tests are shown in *Figure 9* and summarized in *Table 5*. The tensile behaviour of a strained thermoplastic elastomer generally depends on the size, shape and concentration of the hard domains, intersegmental interactions within the hard domains and the ability of the soft segments to crystallize under strain. The PTMO based block copolymer, which contains 27 wt% hard segments in hard domains, possesses the highest Young's modulus and tensile properties. The PBD-based polyurethane contains a similar weight fraction of hard segments in the hard phase as the PTMO-based polymer. However, the noncrystallizable polybutadiene based copolymer which contains the least amount of hard segments in the soft phase possesses a lower tensile strength than PTMO based material and the lowest Young's modulus among the materials tested. The PPO and PEO based block copolymers which contain a hard domain fraction comparable to the PTMO and PBD based materials, exhibit low elongation and strength. This may be ascribed to a lower degree of ordering of their hard segments compared to the PTMO or PBD based elastomers. This ordering which is seen in the d.s.c. traces of *Figure 7* allows for more effective hard domain reinforcement.

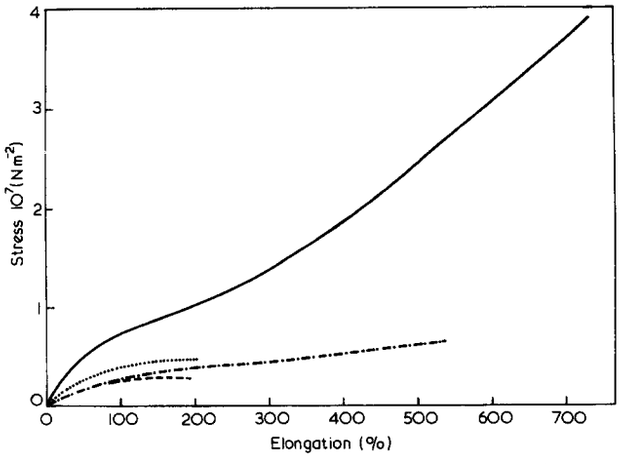

Figure 9 Stress–strain curves for the polyurethane block copolymers with varying soft segment chemistry (PBD, PTMO, PPO and PEO). ——, H_3-PTMO; ·····, H_3-PPO; –·–·–, H_3-PBD, – – –, H_3-PEO

Table 5 Tensile properties of the model polyurethane block copolymers

Sample	Young's modulus (MPa)	σ_b (MPa)	ϵ_b (%)
H_3–PBD	3.88	6.22	528
H_3–PTMO	23.49	39.62	733
H_3–PPO	10.85	3.50	208
H_3–PEO	7.94	2.88	192

CONCLUSIONS

Segmental compatibility has been investigated in both blend and block copolymer urethane systems. The segmented block copolymers were formed by linking the various soft segments with 3 moles of MDI and 2 moles of butane diol in a solution polymerization.

The same oligomeric hard segment, with its chain ends reacted with ethanol, was used as the urethane component in the blends. The soft segments used for both the blend and block copolymer systems include PEO, PPO, PTMO and PBD where only PEO and PTMO are crystallizable, and PBD is the only polyol which has no possibility to form hydrogen bonds with the hard segments. The morphology of the blend systems primarily depends on the crystallizability of the soft segments used, while the morphology of the block copolymer is governed by the thermodynamics of microphase separation which are determined by the molecular interactions between the hard and soft segments.

D.s.c. studies reveal that blends of H_3 and PEO give rise to a eutectic composition at a weight ratio of $\approx 20/80$ (H_3/PEO) with a $T_{m,e} = 34$°C. Blends of H_3 and PTMO also form a eutectic at about $\approx 20/80$ (H_3/PTMO), with a $T_{m,e} = 10$°C. In contrast to the PEO and PTMO systems, both PPO and PBD are intrinsically amorphous compounds and form crystalline–amorphous phase diagrams in blends with H_3. Based on the melting point depression, the interaction densities of H_3/polyol pairs at their melting point, derived using Scott's equation, were found to be $B_{H_3\text{-PEO}} = -0.20\,\text{cal cm}^{-3}$, $B_{H_3\text{-PTMO}} = -0.17\,\text{cal cm}^{-3}$, $B_{H_3\text{-PPO}} = 1.39\,\text{cal cm}^{-3}$ and $B_{H_3\text{-PBD}} = 1.43\,\text{cal cm}^{-3}$. This suggests that the miscibility of H_3 and polyols at the melting point of H_3 appears in the order of PEO > PTMO > PPO > PBD. Compared with previous work[15], the present study indicates that compatibility between the hard segment and soft segment is reduced by extending the hard segment length in the blends. This observation is supported by the Flory–Huggins theory[38] which shows how an increase in the degree of polymerization results in a decrease in the entropy of mixing and thus would lower the intersegmental compatibility.

In the case of block copolymers, both the dynamic mechanical analysis and tensile property study indicate that the block copolymerization of each polyol results in two phase termoplastic elastomers. Both d.s.c. and i.r. analyses show that the extent of phase separation is dependent on the soft segment used and increases in the order of PEO > PPO > PTMO > PBD. This can be explained by the change in the ether content of the polyol, which ranges from zero in PBD to a rather high level in

the PEO-based polyurehtane. The miscibility of the hard and soft segments in the amorphous phase follows the predictions of Hilderbrand's solubility parameter concept.

The melting points of the hard segments in both PTMO- and PBD-based polyurethanes are much lower than the melting points of H_3 in the corresponding blends. As the hard segments are of the same average length in both cases, the difference in T_m is probably due to the lamella size or domain ordering. It is generally accepted that the diffusion of hard segments in block polymers is restricted by the hard–soft segment junction points. This should slow the hard segment crystallization rate in the block polymers relative to the blends. Another effect of the mixing of hard segments in the soft segment phase is the lower diffusion rate for the urethane units caused by the increase in the viscosity of the soft segment-rich phase. This further limits the rate of hard segment coagulation in the process of microphase separation, particularly when the soft segment phase T_g is close to the sample storage temperature. It is thus not surprising that the block copolymer and blend systems should exhibit different overall morphology and different urethane phase melting characteristics.

REFERENCES

1 Paik Sung, C. S., Smith, T. W. and Sung, N. H. *Macromolecules* 1980, **13**, 117
2 Van Bogart, J. W. C., Lilaonitkul, A., Lerner, L. E. and Cooper, S. L. *J. Macromol. Sci.-Phys.* 1980, **17**, 267
3 Van Bogart, J. W. C., Gibson, P. E. and Cooper, S. L. *J. Polym. Sci.–Phys.* 1983, **21**, 65
4 Paik Sung, C. S. and Schneider, N. S. *J. Mat. Sci.* 1978, **13**, 1689
5 Hu, C. B., Ward, Jr., R. S. and Schneider, N. S. *J. Appl. Polym. Sci.* 1982, **27**, 2167
6 Ophir, Z. and Wilkes, G. L. *J. Polym. Sci.–Phys.* 1980, **18**, 1469
7 Seymour, R. W. and Cooper, S. L. *J. Polym. Sci.* 1971, **B9**, 689
8 Srichatrapimuk, V. W. and Cooper, S. L. *J. Macromol. Sci.–Phys.* 1978, **15**, 267
9 Paik Sung, C. S., Hu, C. B. and Wu, C. S. *Macromolecules* 1980, **13**, 111
10 Speckhard, T. A., Ver Strate, G., Gibson, P. E. and Cooper, S. L. *Polym. Eng. Sci.* 1983, **23**, 337
11 Brunette, C. M., Hsu, S. L., Rossman, M., MacKnight, W. J. and Schneider, N. S. *Polym. Eng. Sci.* 1981, **21**, 668
12 Clough, S. B., Schneider, N. S. and King, A. O. *J. Macromol. Sci.–Phys.* 1968, **B2**, 553
13 Van Bogart, J. W. C., Lilaonitkul, A. and Cooper, S. L. *Am. Chem. Soc., Adv. Chem. Ser.* 1979, **176**, 3
14 Chang, Y.-J. P. and Wilkes, G. L. *J. Polym. Sci. Edn.* 1975, **13**, 455
15 Hwang, K. K. S., Hemker, D. J. and Cooper, S. L. submitted to *Macromolecules*, accepted for publication
16 Lockwood, R. J. and Alberino, L. M. *Am. Chem. Soc. Organic Coatings Prepr.* 1980, **43**, 899
17 Lin, S. B., Hwang, K. K. S., Wu, G. and Cooper, S. L. submitted to *Macromolecules*
18 Nishi, T. *J. Macromol. Sci.–Phys.* 1980, **B17**(3), 517
19 Scott, R. L. *J. Chem. Phys.* 1949, **17**, 279
20 Olabisi, O., Robeson, L. M. and Shaw, M. T. 'Polymer–Polymer Miscibility' Academic Press, New York, 1979
21 Hwang, K. K. S., Wu, G., Lin, S. B. and Cooper, S. L. *J. Polym. Sci. Polym. Chem. Edn.*, accepted for publication
22 Krause, S. *J. Polym. Sci.* 1969, **A-2**, 249
23 Meier, D. J. *J. Macromol. Sci.–Phys.* 1980, **17**, 181
24 Boyarchuk, Y. M., Rappoport, L. Ya, Nikitin, V. N. and Apukhtina, N. P. *Polym. Sci. USSR* 1965, 7, 859
25 Seymour, R. W., Estes, G. M. and Cooper, S. L. *Macromolecules* 1970, **3**, 579
26 Barrow, G. M. *J. Chem. Phys.* 1954, **21**, 2008
27 Schneider, N. C. and Paik Sung, C. S. *Polym. Eng. Sci.* 1977, **17**, 73
28 Fedors, R. F. *J. Polym. Sci., Phys.* 1968, **B2**, 115
29 Brandrup, J. and Immergut, E. H. (Eds.) 'Polymer Handbook' 2nd Edn., IV–337, Wiley, New York, 1975
30 *Ibid.* IV–45
31 Kojima, H., Nishimura, H. and Funaki, M. *Reports Res. Lab., Asahi Glass Co., Ltd.* 1981, **31**, 109
32 Tobolsky, A. V. and Mark, H. F. (Eds.) 'Polymer Science and Materials' Wiley–Interscience, New York, 1971
33 Huh, D. S. and Cooper, S. L. *Polym. Eng. Sci.* 1971, **11**, 369
34 Yang, C. Z., Hwang, K. K. S. and Cooper, S. L. *Makromol. Chem.* 1983, **184**, 651
35 Meier, D. J. *Am. Chem. Soc., Div. Polym. Chem. Preprints* 1970, **11**, 400
36 Helfand, E. *Macromolecules* 1975, **8**, 552
37 Blackwell, J. and Nagarajan, M. R. *Polymer* 1981, **22**, 200
38 Flory, P. J. 'Principles of Polymer Chemistry', Cornell University Press, 1953